



VARIABILITY AND COUPLING OF SEA CURRENT VELOCITY, ICE DRIFT AND WIND IN THE PECHORA SEA DURING THE EXPERIMENT OF 2001-2003

N.A. Sukhikh, G.K. Zubakin, N.E. Ivanov, A.V. Nesterov, Y.P. Gudoshnikov
AARI (Arctic and Antarctic Research Institute), St. Petersburg, Russia

ABSTRACT

Data analysis was performed per seasons, distinguished for open water and ice of various thickness, concentration and ridging intensity. Variability characteristics of vectors of currents, drift and wind and their coupling were obtained on the basis of vector-algebraic method of probability analysis of Euclidean vectors, correlation method of K. Watanabe - Z.M. Gudkovich and system of indices of vector correlation in form of invariants. Results of spectral analysis in ranges from seasonal to diurnal, assessment of contribution of tidal and wind components to summary variation, distribution of probabilities and its main points, vector correlation of drift with wind and currents at different horizons, wind coefficients and angle of deviation of drift from wind are presented.

INTRODUCTION

The first part of this study (Zubakin et al., 2015) provides an extensive analysis of the hydrometeorological conditions in the area of Pechora Sea in 2001-2003. The hypotheses of the processes are formed and they are studied by statistic and probabilistic methods in the second part of the study.

This (second) part is dedicated to evaluation of variability and coupling of wind, currents and ice drift velocities according to measurement data, obtained during 2001 – 2003 in the Pechora Sea from two submerged autonomous subsurface buoy stations (ASBS) (Zubakin et al., 2015). The analysis was performed per seasons, distinguished for open water and ice of various thickness and concentration. Some results, obtained during the analysis of variability of currents and drift velocities in the Pechora Sea, are presented in paper (Sukhikh et al., 2014). Thus, the second part of this study is linked with the first part.

Previously the data of 2-year experiment had been used only in a fragmentary manner. This article is a first attempt to make a thorough analysis of the obtained data with the help of advanced methods.

STATISTICAL CHARACTERISTICS OF VARIABILITY AND COUPLING OF CURRENTS, ICE DRIFT AND WIND

Velocities of currents, drift and wind are considered as Euclidean vectors \vec{V} with module V , directions φ , and Cartesian projections V_x , V_y , which sum up as per parallelogram law, transform of coordinates during rotation and adopt three types of multiplication – scalar multiplication, vector multiplication and tensor multiplication (Kochin, 1961).

Statistical variability analysis was performed using vectorial - algebraic method (Belyshev et al., 1983). Straightforward characteristic of \vec{V} as vector random variable is bidimensional distribution of variables $f(V, \varphi)$ by modulus V and direction φ , and one-dimensional distribution of $f(V)$ and $f(\varphi)$. Their critical point is mean vector $\bar{m}_{\vec{V}}$ and dispersion tensor

$$D_{\vec{V}} = M\{(\vec{V} - \bar{m}_{\vec{V}}) \otimes (\vec{V} - \bar{m}_{\vec{V}})\} = \begin{pmatrix} \lambda_1 & 0 \\ 0 & \lambda_2 \end{pmatrix}, \quad (1)$$

where \otimes stands for tensor product function. In order to put symmetric tensor $D_{\vec{V}}$ in diagonalized form (1), the original coordinates were turned about angle $\alpha \pm 180^\circ$, which corresponds to direction of maximum variability \vec{V} . Scalar numbers $\lambda_{1,2}$ are invariants of the tensor (1), i.e. do not depend on orientation of original coordinates. They characterize distribution of dispersion in orthogonal directions and their combinations are invariants as well. Linear invariant $I_1 = \lambda_1 + \lambda_2$ describe full dispersion model (due to joint variations of modulus and direction).

Mean-square velocity deviation (MSVD) may be represented as ellipse $\sigma_{\vec{V}}$ with semi-axis $\sqrt{\lambda_{1,2}}$, with elongation, which describes invariant $\chi = \lambda_2/\lambda_1$. Further values of invariants $\sqrt{I_1}$ and $\sqrt{\lambda_{1,2}}$ are indicated without radical symbol.

Following the method (Zubakin, 1987; Gudkovich and Doronin, 2001), mean value of \vec{V} , root-mean-square deviation σ_V and maximum value V_{\max} of scalar velocity modulus V were also used. That is why per cent ratio $\gamma_d = (1 - I_1/\sigma_V) \times 100\%$ of full vector MSVD I_1 and MSVD velocity scalar modulus gives approximate input of direction variations into general variability. Ratio $v = I_1/m_{\vec{V}}$ of invariant I_1 of the tensor (1) to modulus $m_{\vec{V}}$ of average velocity vector is a vector form of variability ratio.

Structure of temporal variability \vec{V} is described by tensor of spectral density $S_{\vec{V}}(\omega)$. Its linear invariant $I_1(\omega)$ describes intensity of full (in relation to modulus and direction) variability, and the index of square invariant $G(\omega)$ shows prevailing clockwise or counter-clockwise rotation. Required and sufficient assumption of no rotation is $\lambda_2(\omega) = 0$, $I_1(\omega) = \lambda_1(\omega)$. Such statistics were already used for description of wind and drift variability for icebergs and ice floes in the North-European Basin of the Arctic Ocean (Zubakin, 1987), in north-eastern part of the Barents Sea (Zubakin et al., 2013 (a, b); Zubakin et al., 2014; Zubakin et al., 2013), wind drift at station “Severnyi Polyus SP -35” (Ivanov et al., 2011) and ice in the Arctic Ocean according to satellite data (Volkov et al, 2012).

Dependence in the system of random vectors \vec{V} and \vec{G} describes asymmetric (as opposed to dispersion tensor) covariance tensor $\text{Cov}_{\vec{V}\vec{G}}$. According to the study (Belyshev et al., 1983)

linear invariant of its symmetric part $I_1^{\vec{V}\vec{G}}$ describes intensity of mutual changes of collinear components \vec{V} and \vec{G} , and invariant $A^{\vec{V}\vec{G}}$ of anti-symmetric part (rotation indicator) describes intensity of mutual orthogonal variations.

As soon as dependence of random vectors is determined by joint variations of their module and directions, correlation is described by a system of factors, rather than a single number.

For this reason factors of collinear $r_{\uparrow\downarrow} = I_1^{\vec{V}\vec{G}} / (I_1^{\vec{V}} \cdot I_1^{\vec{G}})$ and orthogonal $r_{\perp} = A^{\vec{V}\vec{G}} / (I_1^{\vec{V}} \cdot I_1^{\vec{G}})$ correlation, determined through invariants of dispersion tensors $D_{\vec{V}}$ and covariation $\text{Cov}_{\vec{V}\vec{G}}$, which complies with corresponding individual determinations of coherency of mutual cross-spectral density of random vector processes (Belyshev et al., 1983), were used in the study (Ivanov, 2014).

Indicator $\mu = (r_{\uparrow\downarrow}^2 + r_{\perp}^2)^{0.5}$ describes full correlation and emphasizes the need for joint analysis of $r_{\uparrow\downarrow}$ and r_{\perp} . In case of independence $r_{\uparrow\downarrow} = r_{\perp} = 0$. Otherwise they take up such various values

within the range of $[-1,1]$, that in case of deterministic dependence $\mu=1$, and in case of stochastic dependence $\mu<1$. If dependence is determined only by variation of module \bar{V} and \bar{G} , then $r_{\perp}=0$, and $r_{\uparrow\downarrow}>0$ subject to simultaneous strengthening (weakening) of both vectors, and $r_{\uparrow\downarrow}<0$ subject to strengthening of one vector and weakening of the other. If $r_{\perp}>0$, vector \bar{V} is turned mainly rightwards from vector \bar{G} and vice versa. In case of $\text{abs}(r_{\uparrow\downarrow})>\text{abs}(r_{\perp})$ angle ψ between vectors \bar{V} and \bar{G} is less than 45° and vice versa.

At the same time indicator μ^2 provides determination of dispersion part, explained by regressional dependence of random vectors. Linear regression of vector \bar{V} on vector \bar{G} was determined by A.M. Obukhov (Obukhov, 1938) as

$$\bar{V} = A_{\bar{V}\bar{G}} \bar{G} + \bar{B}_{\bar{V}\bar{G}}, \quad (2)$$

Where regression coefficient $A_{\bar{V}\bar{G}}$, and intercept term $\bar{B}_{\bar{V}\bar{G}}$ is a vector. The formula (2) takes into consideration joint effect of wind on the ice drift and wind-drift current.

Main components of currents' and ice drifts' velocities in the Arctic Ocean are the tidal and non-tidal components. From earlier studies (Zubakin, 1987) it became to our knowledge, that tidal component reaches about 50% of general dispersion. The tidal component was distinguished by precomputation on harmonic constants of major tidal surge, which were determined by least square method (Voinov, 1999).

For the non-tidal component of currents and drift their wind-dependence can be described by linear regression of vector \bar{V} on vector \bar{G} , determined by A.M. Obukhov (Obukhov, 1938) as

$$\bar{V} = A_{\bar{V}\bar{G}} \bar{G} + \bar{B}_{\bar{V}\bar{G}}, \quad (2)$$

Where regression coefficient is $A_{\bar{V}\bar{G}}$, and intercept term $\bar{B}_{\bar{V}\bar{G}}$ is a vector.

Whereas there are "pure wind" and "non-wind" components distinguished in non-tidal component. Correlation method of K. Vatanabe – Z.M. Gudkovich (Gudkovich and Doronin, 2001) was used in order to separate them. Pure wind currents and drift are conditional upon local wind. They were determined using formula (2), where intercept term $\bar{B}_{\bar{V}\bar{G}}$ equals to 0, and tensor components $A_{\bar{V}\bar{G}}$ are calculated per wind and current (or drift) measurements.

Non-wind-driven currents and drift \bar{U} do not depend on local wind. They are formed in the process of conformation of water density field with wind circulation. That is why for some periods from several weeks to a season they are deemed to be constant. Then this constant velocity will be determined by difference of average velocities of aggregate and wind-induced motion

$$\bar{C} = \bar{m}_{\bar{V}} - \bar{m}_{\bar{U}} \quad (3)$$

Another characteristic of drift velocity coupling with wind is the wind coefficient and the angle of deviation. These are specifically important for future calculating and forecasting during fulfillment of ice management tasks. In the studies (Gudkovich and Doronin, 2001; Thorndike and Colony, 1982) these were determined by wind velocity and measured total drift. In the studies (Zubakin et al, 2013(b); Zubakin et al, 2014; Zubakin, 2013) and hereunder, taking into consideration the formula (3) these were determined by wind drift \bar{U} and by wind value \bar{G} as $k=U/G$, $\psi=\varphi_{\bar{U}}-\varphi_{\bar{G}}$.

DATA

Currents and Drift

Analysis was performed for aggregate velocity values and their non-tidal components. Tidal components were distinguished as per harmonic constants (Voinov, 1999). Measurement

resolution was 10 minutes. As soon as during 1 hour data smoothing, regardless of season and any particular horizon, dispersion reduces less than by 5%, hourly average velocity values were used. Distance between ASBS-1 and ASBS-2 is about 117 km. For this reason analysis of spatial coupling was performed using daily average data.

Wind

In cases when no direct measurements were available, the geostrophic wind was used. Fields P (Air Pressure) from reanalysis of NCEP (Kalnay et al., 1996) were used from website of AARI spacing 2.5° latitude and longitude with 6 hour resolution. Values \bar{G} in grid nodes were interpolated into device location point. For compossibility with currents and drift the “towards” wind direction was adopted.

DISCUSSION

Variability of currents \bar{V} , ice drift \bar{W} and variability of wind \bar{G} is presented in data of analysis of variance and spectral analysis, distributions of variables and its points. The coupling \bar{V} measured from diverse horizons and between \bar{W} and \bar{G} is presented by vector correlation indices. Wind coefficients and angles of deviation for \bar{W} and \bar{G} based on models of vector random variable (VRV) and the vector random process (VRP) are also stated.

According to the first part of the work (Zubakin et al., 2015) the year was divided into 9 calendar seasons (season code and 2 last digits of year): SUM01 2/IX-30/X, PRW01 31/X-29/XII, WIN02 30/XII-8/V, SPR02 9/V-3/VIII, SUM02 4/VIII-15/X, PRW02 16/X-23/XII, WIN03 24/XII-1/V, SPR03 2/V-9/VIII, and SUM03 10/VIII-1/X.

Variability of Currents, Ice Drift and Wind

Analysis of Variance and Spatial Coupling

Measured currents and ice drift have discretization of 10 minutes. When shifting to 1 h data smoothing, the relative decrease in the total variance is negligible - $\gamma_D \geq 0.97$. Therefore, hourly average values were used in the analysis. From now on γ_* - is a ratio of invariants I_1 of corresponding tensors $D_{\bar{V}}$.

The article (Zubakin et al., 2015) states that wind and tidal flow are the key factors that determine dynamics of water masses and ice; the tidal component explains up to 50% of the total variance. Vertical profiles $\gamma_{nt}(z)$ of relative variance of the non-tidal component of currents (relative to the total variance) in figure 1 were obtained in both measurements points for 9 seasons at the all horizons. Differences by depth z , seasonal and spatial contrasts of γ_{nt} values are rather small, despite considerable differences between absolute values of overall vector variance I_1 . Let's just note some decrease in γ_{nt} in ASBS-2 as compared to ASBS-1 during winter seasons (WIN-03, 04). The probable reason for this is that ASBS-2 is located much closer to the fast ice edge, than ASBS-1.

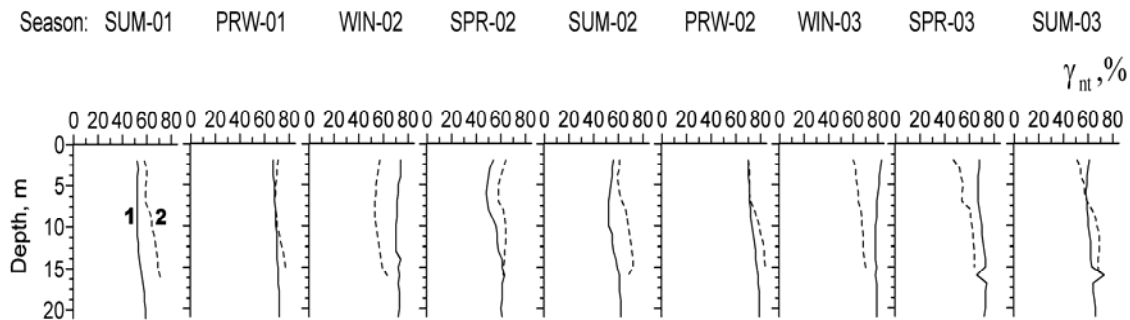


Figure 1. Relative variance of the non-tidal component of current velocities in ASBS-1 (1) and ASBS-2 (2) measurement points.

Ice drift evaluation results are much the same as for currents. For ASBS-1, during winter seasons WIN-02 and WIN-03, γ_{nt} made 70% and 80%; for ASBS-2 in WIN-02 $\gamma_{nt} = 55\%$. The said data confirm that tidal and wind elements make an essential contribution to general dynamics of water masses and ice.

Let's consider spatial coupling. The distance between ASBS-1 and ASBS-2 is about 120 km. Therefore spatial correlation between currents \bar{V} and ice drift \bar{W} is determined by daily average data. When shifting from 1h data smoothing to 24 h data smoothing, the overall dispersion I_1 of current velocities \bar{V} and ice drift \bar{W} decreases only by 15-25%.

Spatial correlation of synchronous daily average \bar{V} values is shown in Table 1 by 8 seasons (exclusive of the first summer season that is not completely provided with measurement data).

Evaluations of overall vector correlation μ and factors $r_{\uparrow\downarrow}$ and r_{\perp} , were made at z horizons (2, 5, 10, and 15 m). Taking into account duration of seasons, the correlation was important in the order of 95%, if $\mu \geq 0.25$, standard error of estimate made 0.05-0.10.

Table 1. The μ indicator and factors of collinear $r_{\uparrow\downarrow}$ and orthogonal r_{\perp} vector correlation of synchronous daily average current velocities in ASBS-1 and ASBS-2.

z, m	Parameter	Season							
		PRW-01	WIN-02	SPR-02	SUM-02	PRW-02	WIN-03	SPR-03	SUM-03
2	μ	0.63	0.15	0.40	0.38	0.67	0.66	0.12	0.24
	$r_{\uparrow\downarrow}$	+0.55	+0.11	+0.38	+0.31	+0.56	+0.45	+0.10	+0.23
	r_{\perp}	-0.46	-0.09	-0.12	-0.20	-0.36	-0.48	-0.07	-0.10
5	μ	0.65	0.75	0.44	0.42	0.76	0.73	0.37	0.43
	$r_{\uparrow\downarrow}$	+0.54	+0.65	+0.36	+0.28	+0.61	+0.48	+0.20	+0.39
	r_{\perp}	-0.38	-0.43	-0.25	-0.31	-0.46	-0.56	-0.31	-0.13
10	μ	0.66	0.76	0.57	0.50	0.81	0.79	0.66	0.48
	$r_{\uparrow\downarrow}$	+0.48	+0.60	+0.40	+0.24	+0.58	+0.49	+0.52	+0.39
	r_{\perp}	-0.44	-0.46	-0.40	-0.45	-0.57	-0.62	-0.37	-0.29
15	μ	0.65	0.75	0.68	0.58	0.82	0.80	0.75	0.58
	$r_{\uparrow\downarrow}$	+0.40	+0.51	+0.42	+0.26	+0.56	+0.49	+0.50	+0.37
	r_{\perp}	-0.51	-0.55	-0.49	-0.52	-0.65	-0.63	-0.54	-0.44

The 24 h data smoothing substantially suppresses tidal oscillation. Correlation of geostrophic wind in ASBS-1 and ASBS-2 is almost no different from 1 - $\mu \cong r_{\uparrow\downarrow} \cong 1$, $r_{\perp} \cong 0$. Nevertheless, the overall correlation μ at the horizon $z=2m$ is weakened. The key factors that make it difficult to evaluate spatial correlation and to determine how the wind and tides influence currents and ice drift, are parameters of the ice cover and flow of the Pechora River (Zubakin et al., 2015). Variability of these factors is time dependent and irregular in space. The overall ice coverage, concentration, thickness of ice, ridging and fast ice are at their maximum from the end of March to the beginning of May. That said, ASBS-2 is much closer to the fast ice edge than ASBS-1. The peak flow of the Pechora River (up to 70% of the yearly total) is annually recorded during the spring flood from May to July. The main part of flow occurs near ASBS-2. From August to October, Pechora water content often increases due to rainfall flood. As a result, in winter 2002 and in spring and summer 2003, correlation at $z=2m$ is negligible, and in spring and summer 2002 is weakened to 0.4. Only in pre-winter

2002-03 and in winter 2003 (when according to Table 3 contained in the work (Zubakin et al., 2015) the negative anomaly of ice coverage in the southwestern Barents Sea was from -10 to -25%) μ value was increased to 0.65.

The key feature of vertical distribution is a sharp increase in μ as depth increases. It was especially evident in winter 2002 (WIN-02) when, as z changed by only 3 m (from 2 to 5 m) correlation strengthened from negligible to $\mu = 0.75$. At a depth of 15 m μ was 0.6-0.8 during for the 8 seasons. The kinematic structure of vector correlation is characterized by signs of factors $r_{\uparrow\downarrow}$ and r_{\perp} , and their absolute values ratio. Table 1 shows that in most seasons (except three cases when μ at a depth of 2 m was negligible) changes related to the depth of collinear correlation are rather small. The increase in μ is almost completely caused by strengthening of negative orthogonal correlation r_{\perp} , and at $z=15$ m r_{\perp} exceeds $r_{\uparrow\downarrow}$ in an absolute value. It means that at a depth exceeding 10 m, currents in ASBS-2 are turned by more than 45° mostly leftwards from currents in ASBS-1.

Spatial correlation of ice drift \vec{W} in ASBS-1 and ASBS-2 from February to May 2002 can be determined using data available. To record the annual change in this interval, evaluations of μ indicator of overall vector correlation and factors of collinear $r_{\uparrow\downarrow}$ and orthogonal r_{\perp} correlation of synchronous daily average drift velocities from February to May are listed in Table 2.

Table 2. The μ indicator and factors of collinear $r_{\uparrow\downarrow}$ and orthogonal r_{\perp} correlation of synchronous daily average drift velocities in ASBS-1 and ASBS-2 in 2002.

Parameter	February	March	April	May
μ	0.71	0.81	0.50	0.23
$r_{\uparrow\downarrow}$	+0.68	+0.80	+0.50	+0.12
r_{\perp}	-0.16	-0.09	-0.07	-0.21

Table 2 shows that from February to April, 2002 the overall vector correlation was important in the order of 95%. From February to March it increased from 0.71 to 0.81, and in April (when the ice cover, including fast ice, is the most developed and the ice keel draft is at its maximum value) remarkably fell to 0.50. In May from the beginning of springtime, the daily average drift correlation in ASBS-1 and ASBS-2 disappeared. The factors of collinear $r_{\uparrow\downarrow}$ correlation are positive and almost keep in scale with μ , and factors of orthogonal r_{\perp} correlation are low negative. It means that spatial coupling of the daily average drift in ASBS-1 and ASBS-2 is almost completely caused by the unidirectional changes in \vec{W} elements collinear to each other, and the average daily drift in ASBS-1 and ASBS-2 is turned by less than 45° leftwards from ASBS-1 on average. Strengthening of spatial correlation for drift as compared to currents on 2 m horizon is related to wind.

Under the time shift of one day and more, spatial correlation of currents and ice drift velocities will weaken dramatically.

Spectral Analysis

Spectral analysis in details are shown in (Sukhikh et al., 2014). Spectra of currents and drift in both measurement points during all seasons and at all depths are qualitatively identical. In

order to specify quantitative peculiarities, spectral function $F(\omega) = \int_{\omega_1}^{\omega_2} I_1(\omega) d\omega$ was used.

Relative variance $F(\omega)/I_1$ was determined in 4 ranges – intra-seasonal (I), intra-monthly (II),

synoptic (III) and diurnal (IV) with periods over 30 days, 10-30 days, 2-10 days and less than 1 day. Consideration in $F(\omega)$ of $I_1(\omega)$ values and width of interval (ω_1, ω_2) enabled to access actual distribution of variance on the distinguished ranges. Assessments of 2-year series of non-tidal currents showed, that over 90% of relative variance is concentrated in three high-frequency ranges II-IV. Correlation between F_{II} , F_{III} and F_{IV} during corresponding seasons at the corresponding depths were about the same. Almost in all cases main contribution to variance is brought by synoptic variability 45-70%, which increases during pre-winter and winter season. Seasonal peculiarities are especially visible in redistribution of variance between ranges F_{II} and F_{IV} . In winter intra-monthly oscillations F_{II} explain 25-35% of variance, and diurnal oscillations F_{IV} only 10%, whereas in summer and spring the correlation is inverse, and during pre-winter contributions to variance of F_{II} and F_{IV} are commensurate. Vertical difference is observed only in spring-summer flow period of Pechora River and related to redistribution of variance in synoptic and diurnal ranges. Thus, in spring 2003 in point ASBS-2 at depth $z=2$ m values F_{III} and F_{IV} made 25% and 60%, and at depth $z=5$ m – 50% and 35%.

Table 3 contains distributions $F(\omega)$ on 4 ranges of non-tidal drift \bar{W} and current \bar{V} at the depth of $z=2$ m. It shows that wind role appears in escalation of synoptic variability (range III) for \bar{W} as compared with \bar{V} . In 2002 difference made 15%, and in 2003 the difference increased up to 25%.

Table 3. Distribution of relative variance (%) of non-tidal components of currents ($z=2$ m) from drift on frequency ranges during winter seasons 2002-03 in points ASBS-1,2.

Year	Parameter	ASBS-1				ASBS-2			
		Range No.				Range No.			
		I	II	III	IV	I	II	III	IV
2002	Drift	8	13	61	18	9	14	60	17
	Current	5	36	45	14	5	27	44	24
2003	Drift	5	7	70	15	-	-	-	-
	Current	5	27	45	21	-	-	-	-

Distribution of Probabilities and its Moments

Main characteristic of currents \bar{V} and drift \bar{W} as VRV is frequency of occurrence $f(V, \varphi)$ on rhumbs and gradations of modulus. Type of distribution $f_V(\bullet)$ on all horizons and $f_W(\bullet)$ is same for each season. Figure 2 shows frequency roses for non-tidal currents in winter 2003 at the depths of 2, 5, and 15 m. Height of rectangles implies velocity modulus (6 gradation levels, graduated scale is presented top left). Length of rectangles shows gradation frequency $f(V, \varphi)$, total length of beams corresponds to frequency of occurrence on rhumbs $f(\varphi)$. Figure 2 demonstrates increased frequency of currents and drift, directed towards east and north-east and reduction of velocity at rhumbs with low frequency $f(\varphi)$.

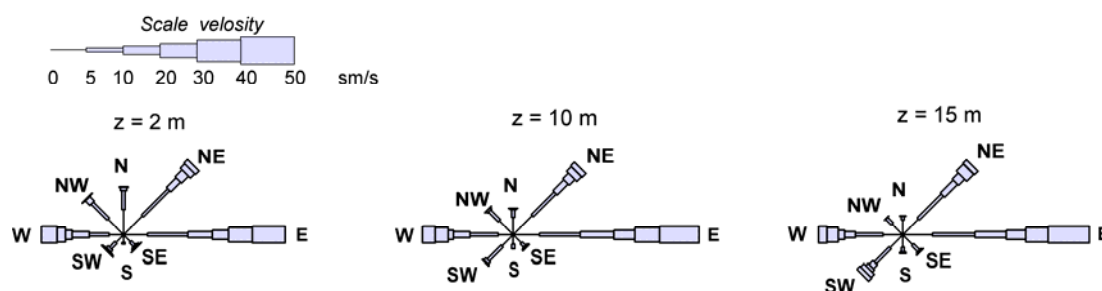


Figure 2. Frequency roses for velocity of non-tidal currents at ASBS-1 in winter 2003 at the horizons of 2, 10 and 15 m.

Considering similarity of drift and currents distribution pattern at various depths for each season, the difference between seasons is considerable in terms of numerous parameters. Velocities of currents and ice drift over 1 m/s were registered from 2001 till 2003. This requires more gradations of velocity modulus as compared to estimations shown on Figure 2. However, due to limited volume of sampling, this will result in statistically unreliable values in numerous cells of distribution tables $f(V, \varphi)$. For this reason, we will review basic distribution moments.

Calculation based on data of the years 2001 - 2003 showed that during all 9 distinguished seasons and at all depths the vector of mean current velocity \bar{m}_V is directed towards north-east. At the same time meridional component at ASBS-2 measurement point was increased as compared to ASBS-1. Same quasi-constancy in time and depth is typical of RMSD ellipse form with invariant $\chi < 1$, which means irregularity in the distribution of variance on directions. Figure 3 shows vertical profiles of mean non-vector velocity of currents \bar{V} and mean-square deviations – non-vector and σ_V and vector I_1 .

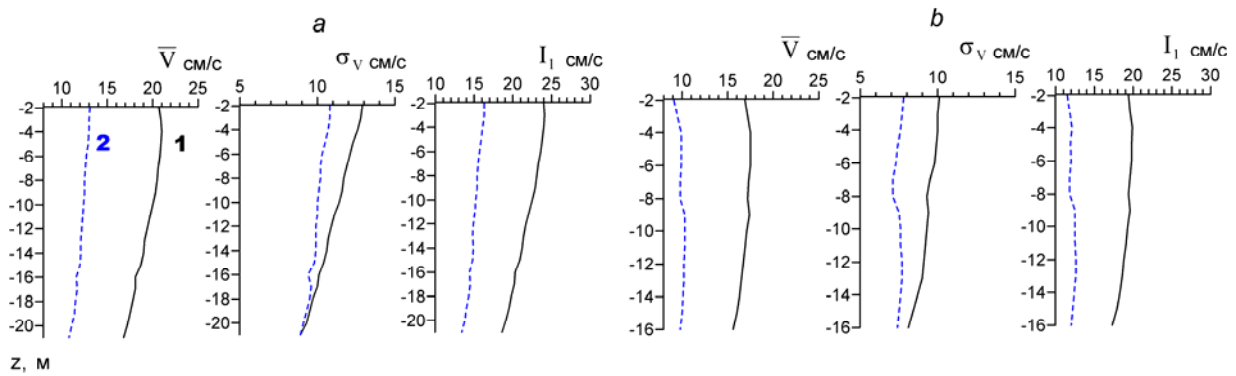


Figure 3. Vertical profiles of distribution moments of velocities of summary current (1) and non-tidal component (2) at ASBS-1 (a) and ASBS-2 (b) measurement points.

Such quasi-homogeneous vertical profiles are typical for all seasons but values of the parameters vary significantly from season to season. Range of their variation in terms of summary currents for ASBS-1,2 measurement points are presented in table 4. It shows that in most cases range of seasonal fluctuations at a fixed horizon exceeds vertical changes during a fixed season. Significant excess of I_1 over σ_V indicates great contribution of variability of speed direction to full vector variance.

Table 4. Range of seasonal fluctuations of velocity parameters of summary currents (cm/s) – mean non-vector velocity \bar{V} , mean-square deviation σ_V and full vector RMSD I_1 .

z, m	ASBS-1			ASBS-2		
	\bar{V}	σ_V	I_1	\bar{V}	σ_V	I_1
2	18.0-25.2	9.1-16.1	19.5-29.7	12.2-21.4	7.8-11.3	14.5-22.2
5	17.8-24.5	9.0-15.4	19.6-28.1	13.0-210.0	8.1-11.0	15.4-23.3
10	18.0-22.3	9.1-14.0	19.5-24.3	14.9-19.5	8.2-11.3	16.4-22.1
15	17.4-21.4	8.6-12.9	19.1-23.6	13.7-18.4	6.6-10.8	14.9-20.2

Ice drift was measured during the period from February till May 2002 at ASBS-1, 2, and at ASBS-1 only in 2003. In order to register seasonal variations of ice cover according to recommendations (Zubakin et al., 2015), the two intervals were distinguished for each year: February – March and April - May. Figure 4 demonstrates combined vectors of mean velocities $\vec{m}_{\bar{v}}$ and ellipses of mean deviation $\sigma_{\bar{v}}$ of geostrophic wind and non-tidal components of drift and currents at the horizons $z=2$, $z=5$ m. Values of mean non-vector velocity \bar{V} , its mean-square deviation σ_v , modulus of mean velocity vector $m_{\bar{v}}$, full mean-square deviation I_1 and relative variance of velocity direction change γ_d are shown in the table 5.

Table 5. Statistics of ice drift for the period February-May in 2002 and in 2003.

Year	Month	ASBS-1					ASBS-2				
		\bar{V} , cm/s	σ_v , cm/s	$m_{\bar{v}}$, cm/s	I_1 , cm/s	γ_d , %	\bar{V} , cm/s	σ_v , cm/s	$m_{\bar{v}}$, cm/s	I_1 , cm/s	γ_d , %
2002	Feb-Mar	11.3	12.8	0.8	17.1	43	13.7	10.6	4.3	16.8	60
	Apr-May	13.1	16.1	3.8	20.4	38	8.4	9.4	2.2	12.5	42
2003	Feb-Mar	24.7	25.0	15.2	31.7	37	-	-	-	-	-
	Apr-May	17.2	17.6	5.3	24.7	46	-	-	-	-	-

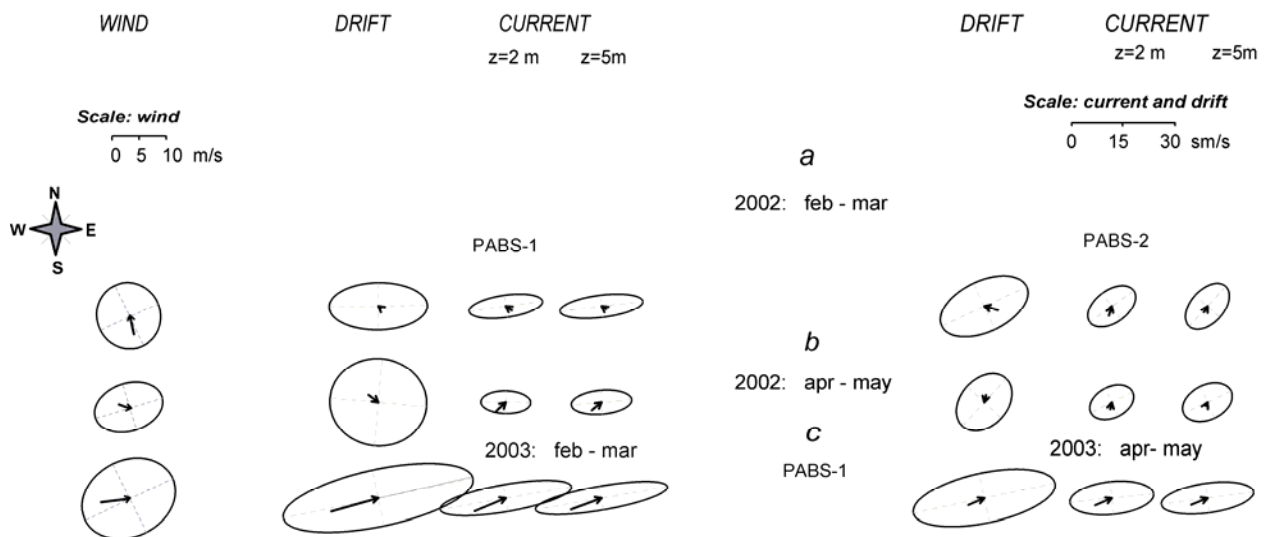


Figure 4. Vectors of mean velocity and ellipses of wind MSD, non-tidal components of currents at horizons $z=2$, $z=5$ m and drift at stations ASBS-1,2 in February-March 2002 (a), April-May 2002 (b) and at station ASBS-1 in February – March and in April-May 2003(c).

Main particulars of drift and currents in February – May 2002 and 2003 are:

- Prevailing orientation of mean velocity and maximum variability towards west-east with strongly elongated ellipse of mean-square deviation;
- High variability – standard deviations are several times greater than mean values;
- Dependence of drift characteristics and currents not only from wind, but also from seasonal ice conditions.

According to the analysis results:

1. During pre-winter and winter of 2002 (seasons PRW01 and WIN02) from $z=2$ m to $z=3$ m a sharp increase V_{max} of summary current with almost unchanged V_{max} of non-tidal component.
2. In spring and summer 2003 (seasons SPR03 and SUM03) in layer from $z=2$ m to $z=5-7$ m

values of V_{\max} of summary current and non-tidal component decreased significantly.

This confirms an assumption that ice cover, river discharge and melt water aggravate assessment of currents and drift, their coupling with wind and distinguishing of tidal component (Zubakin et al., 2015). Considering this fact, another moment should be noted. The strongest wind (37-39 m/s) was registered in winter 2003, and in spring in reduced to 22 m/s. At the same time V_{\max} at ASBS-1 increased from winter to spring about 30 cm/s within upper 5 meter layer.

Maximum values of velocities W_{\max} of summary (a), non-tidal drift (b) and wind G_{\max} from February till May 2002 at ASBS-1 and 2 and in 2003 at ASBS-1 are presented in table 6 per month.

Table 6. Maximum velocities of summary (a), non-tidal (b) drift W_{\max} , cm/s at ASBS-1 and 2 and wind G_{\max} , m/s per month from February till May.

Point	-	-	Year: 2002				Year: 2003			
			Month				Month			
			Feb	Mar	Apr	May	Feb	Mar	Apr	May
Drift - ASBS-1	W_{\max}	a	71	77	71	119	108	133	64	112
		b	60	65	71	101	99	127	70	116
Drift - ASBS-2	W_{\max}	a	60	48	45	108	-	-	-	-
		b	59	40	29	83	-	-	-	-
Wind	G_{\max}		27	21	21	24	30	37	26	22

Table 6 shows that during measurement period very high ice drift velocities were registered – up to 135 cm/s and 125 cm/s for summary and non-wind drift. For the period February - April the fastest drift was registered in March 2003, together with the strongest wind – 37 m/s. In May degradation of ice cover takes place and discharge of Pechora River increases sharply. During this period in 2002 (ASBS-1 and 2) and in 2003 (ASBS-1) value W_{\max} increases sharply as compared to April, but this was not accompanied by increase of wind G_{\max} .

Coupling of Current, Ice Drift and Wind Velocities

Distinguishing of relations between wind, ice drift and currents in south-eastern part of the Pechora Sea was complicated by a number of factors. Main peculiarity is the area orography – shallowness, close vicinity of the shore and the island. This influences seasonal peculiarities as well. The fast ice is primary seasonal feature, which shifts the shallow area boundaries when adjoining with ridge keels and hummocks, and distorts “classic” deviation of drift from the wind. During the experiment ASBS-2 was located much closer to the fast ice edge, as compared to ASBS-1 station. Another important seasonal factor is the flow of Pechora River. During springtime high flood from May till July the major part of river flow is brought up near ASBS-2. In August – October there are often rainfall floods.

Coupling of wind with current and drift was determined as per recommendations (Zubakin et al., 2015) considering seasonal variation. Tidal currents and drift in shallow Pechora Sea are mainly barotropic. Non-periodic variability is mainly determined by wind. Wind coupling with non-tidal components of currents and drift is characterized by vector correlation indicator μ , factors r_{τ} , r_{\perp} , wind coefficient k and drift deviation angle from the wind ψ .

Values $k = U/G$ and $\psi = \varphi_{\bar{U}} - \varphi_{\bar{G}}$ were determined from “pure wind” drift \bar{U} , distinguished from total non-tidal drift \bar{V} using the formulas (2-3). Period of maximum possible ice load is

extremely important for design and further operation of hydrotechnical structures in Arctic region. Table 7 contains estimates for wind and drift coupling μ , $r_{\uparrow\downarrow}$, r_{\perp} , k , ψ per month from February till May at ASBS-1, 2 stations.

Table 7. Parameters of dependence of non-tidal drift from wind – indicator and factors of collinear and orthogonal correlation, wind coefficients and deviation angles.

Month	μ	$r_{\uparrow\downarrow}$	r_{\perp}	k	ψ
Measurement point and year - ASBS-2, 2002					
Feb.	0.78	+0.68	-0.46	0.015	-21°
Mar.	0.75	+0.70	-0.28	0.011	-20°
Apr.	0.55	+0.51	-0.21	0.009	-17°
May.	0.40	+0.22	-0.32	0.010	-29°
Measurement point and year - ASBS-1, 2002					
Feb.	0.68	+0.65	-0.16	0.008	-18°
Mar.	0.65	+0.63	-0.19	0.013	-15°
Apr.	0.63	+0.61	-0.11	0.011	-10°
May.	0.50	+0.47	-0.03	0.013	-15°
Measurement point and year - ASBS-1, 2003					
Feb.	0.80	+0.79	-0.08	0.018	-6°
Mar.	0.79	+0.79	-0.05	0.018	-8°
Apr.	0.65	+0.64	-0.05	0.014	-7°
May.	0.67	+0.65	-0.13	0.021	-22°

Table 7 enables to make several preliminary (due to limited number of years) conclusions of physical character.

- General correlation of μ in April and May decreases as compared with February and March. Especially this was noticeable at ASBS-2 station in 2002. Possible reason of μ reduction from 0.75 to 0.55 from March to April is increasing ridge keel draft and close vicinity of ASBS-2 to the fast ice and associated rafting ice. The most probable reason of correlation weakening to 0.40 in May as compared to April is the flow of Pechora River.
- Signs and correlations of absolute values of $r_{\uparrow\downarrow}$ and r_{\perp} characterize kinematic structure of vector correlation. Collinear correlation $r_{\uparrow\downarrow}$ is always positive and exceeds (except for May 2002 at ASBS-2 station) the orthogonal correlation per absolute value. This means, that dependence of drift from wind is first of all determined by one-directional variations of their velocities. This was specifically noticeable in February-March 2003, when relatively strong winds with stable directions prevail, and total correlation reached 0.8, which was almost fully determined by $r_{\uparrow\downarrow}$ factor.
- It is crucially important that orthogonal correlation in all cases is negative. This means, that in the reviewed situations the drift is turned to the left from the wind. Indeed, all angles ψ in table 7 are negative. Increment of negative deviation ψ at ASBS-2 should be noted separately. This corresponds to data of (Zubakin, 1987) showed at figure 3 of the article (Zubakin et al., 2015).
- Wind coefficients k for geostrophic wind and drift in 2002 made 0.008-0.015, and in 2003 they increased up to 0.018-0.021. Considering complicated orography of the area this does not conflict with results obtained earlier.

ACKNOWLEDGEMENTS

The authors acknowledge Dr. I.V. Buzin for the help in the edition, translation and preparation of the manuscript.

REFERENCES

- Belyshev, A.P., Klevantsov, Yu.P., Rozhkov, V.A., 1983. Probability analysis of marine currents. L., Hydrometeoizdat, 264 pp.
- Gudkovich, Z.M., Doronin, Yu.P., 2001. Drift of sea ice. Saint-Petersburg, Hydrometeoizdat, 110 pp.
- Ivanov, N.E., 2004. Regarding characteristics of correlations between wind speeds, sea currents and ice drift. Meteorology and hydrology, No. 8, pp. 61-72.
- Ivanov, N.E., Visnevskiy, A. A., Sokolov, V.T., 2011. Wind drift of station "The North Pole SP-35". Arctic and Antarctic Problems, No. 1, pp. 5-21.
- Kalnay, E., 1996. The NCEP/NCAR 40-Year Reanalysis Project. Bul Amer Meteor Soc, 77, pp. 437-470.
- Kochin, N.E., 1961. Vector analysis and basic tensor analysis. M., AN USSR Publishing house, 425 pp.
- Obukhov, A.M., 1938. Normal correlation of vectors. AN USSR News, No. 3, pp. 339 – 369.
- Sukhikh, N.A., Zubakin, G.K., Ivanov, N.E., Nesterov, A.V., 2014. Structure of currents and ice drift in the Pechora Sea. Papers of VIII International research-to-practice conference "Dynamics and thermal features of rivers, water basins and coastal areas of seas", Moscow, RUDN, 24-27 November 2014. M. Peoples' Friendship University of Russia, pp. 248-260.
- Thorndike, A.S, Colony, R., 1982. Sea Ice Motion in Response to Geostrophic Winds, Journal of Geophysical Res, Vol 87, No C8, pp. 5845-5852.
- Voinov, G.N., 1999. Tide in the Kara Sea. Saint-Petersburg, pp. 110.
- Volkov, V.A., Ivanov, N.E., Demchev, D.M., 2012. Use of vectorial-algebraic method in research on marine ice drift. XV Glaciological symposium "Present Day Variability of the Earth cryosphere".
- Volkov, V.A., Ivanov, N.E. and Demchev, D.M., 2012. Application of a vectorial-algebraic method for investigation of spatial-temporal variability of sea ice drift and validation of model calculations in the Arctic Ocean. Journal of Operational Oceanography, Volume 5, No 2, pp. 61-71.
- Watanabe, K., 1962. Drift velocities of the ice measures from air and current introduced components. – Study on sea ice in the Okhotsk (II). Oceanogr. Mag, vol. 14, No. 11, pp. 23-37.
- Zubakin, G.K., 1987. Large-scale variability of condition of ice cover of North-European Basin. L., Hydrometeoizdat, 160 pp.
- Zubakin, G.K., Ivanov, N.E., 2014. Drift of icebergs and ice floes in north-eastern part of the Barents Sea. Meteorology and hydrology, No. 10, pp. 65-78.
- Zubakin, G.K., Ivanov, N.E., Nesterov, A.V., 2013. GPS-Measured Drift of Icebergs in the North-Eastern Barents Sea and its Correlation with Fields of Atmospheric Pressure. Proceedings of the Twenty-third International Offshore and Polar Engineering Anchorage, Alaska, USA, pp. 1072-1079.
- Zubakin, G.K., Ivanov, N.E., Nesterov, A.V., 2013. Assessment of iceberg drift speed and atmospheric pressure variability and gradient of atmospheric pressure in the north-eastern part of the Barents Sea. Arctic and Antarctic Problems, No. 3(97), pp. 65-78.
- Zubakin, G.K., Ivanov, N.E., Nesterov, A.V., 2013. Coupling of iceberg drift with atmospheric pressure field in north-eastern part of the Barents Sea. Arctic and Antarctic Problems, No. 2(96), pp. 26-41.
- Zubakin, G.K., Gudoshnikov, Yu.P., Ivanov, N.E., Nesterov, A.V., Sukhikh, N.A., 2015. Hydrometeorological and ice conditions in the Pechora Sea during experiment in 2001-2003 (included herein).
- Zubov, N.N., 1945. Arctic ice. M., Publisher - Glavsevmorput', 360 pp.